MODELLING OF PARTIAL DEBONDING OF DUCTILE PARTICLES FROM BRITTLE MATRIX IN CRACK BRIDGING ZONE

R. URBIŠ AND M. KOTOUL
Department of Solid Mechanics, Brno University of Technology,
Technická 2, 616 69 Brno, Czech Republic

ABSTRACT

The restraining effect of second-phase particles on an advancing crack front is analyzed. The stress-crack opening displacement relationship relies upon the constant volume plastic flow of the particles according to the model suggested recently by Rubinstein and Wang [1]. This model incorporates in a certain way also the matrix/particle interface properties. The particles are allowed to deform using several different patterns which correspond to the particular strength of the matrix/particle interface. Contrary to Rubinstein and Wang's work the triaxiality of the stress state within particles and strain hardening effects are considered and their impacts on the critical crack opening displacement are investigated. The toughness increase is predicted for several combinations of micromechanical parameters of composite system and the strain hardening exponent of second-phase particles.

KEYWORDS

Fracture toughness, particulate composites, bridged cracks, strongly singular integral equations.

INTRODUTION

In certain materials, the opening of a crack may be opposed by physical bridges between the crack faces. One example is ceramics containing ductile metal particles (particulate-reinforced ceramics). The restraining effect of the second-phase particles on an advancing crack front is the basic for a toughness increment. Phenomenologically, a toughening mechanism is described as follows: an existing initial flaw in a brittle matrix propagates and, because of stress concentration around the particles, circumvents the ductile particles which are thus left intact behind the crack tip and act as bridges between the opposing faces of the crack. In the course of further crack opening they deform plastically and finally, after reaching a critical elongation, they fail by ductile rupture. These particles also prevent excessive crack opening and thereby reduce the crack driving force at the crack tip. Since the crack driving force must reach a critical value for further crack extension, this requires a higher value of the applied stress for crack propagation than would be necessary in the absence of particles. Stretched ductile particles (ligaments), e.g. Al particles in Al_2O_3/Al systems or Co enclaves in WC/Co composites, are detected at considerable distance l_p behind the crack tip. It justifies the application of the term multiligament zone. The basics of the mechanism of fracture toughness enhancement in brittle matrix composites with distributed ductile particles were analyzed in the literature, e.g. [2]-[6].

However, in order for the process described to take place, certain conditions need to be satisfied. First, the deflection of the crack towards the adjacent particle and stress concentration around the particle in the plane perpendicular to the applied load are possible only if the stiffness of the particles is less than that of the matrix. Otherwise, if the particles are stiffer than the matrix, the crack would be repelled by the particle and, as a consequence, the crack would remain entirely in the matrix and there would be no significant influence of the particles on the toughness of the material. The attraction mechanism of the crack tip to the particles thus ensures that the crack path is formed through a number of ductile particles. Secondly, the particles's ductility alone is not sufficient for any significant improvement in toughness. It is observed that the quality of the matrix/particle interface also becomes of great importance because it strongly influences the particle deformation pattern. Specifically, some optimum interface debonding is needed to remove the geometric constraint and allow the particles to deform plastically in a significant part of their volume. For example, if the matrix/particle interface is very strong and the particles do not debond, then the plastic flow within particles would remain localized in a thin layer along the crack plane. The critical crack opening displacement Δ_C corresponding to the particle rupture would be relatively small and there would not be a significant increase in the composite toughness. On the other side, for very low matrix/particle interface strength, the particle would readily debond and there would be no crack surface bridging action and, again, no significant improvement in toughness. The significance of the effect associated with the matrix/particle interface was emphasized by Tvergaard [7], [8] using the finite element analysis of the plastic flow within the particle, as well as Sigl *et al.* [9] and Venkateswara Rao *et al.* [10] using experimental evidence and physical observations of the process.

An analytical approach, allowing detailed calculation of the development of the fracture toughness during loading, was presented by Rubinstein and Wang [1]. Their modelling approach is based on a discrete particle distribution. Particles are assumed to be elastic-ideally plastic and allowed to deform using several different patterns which correspond to the particular strength of the matrix/particle interface. The deformation patterns are simplified versions of those obtained by Tvergaard [7] using finite element computations, as illustrated in Fig. 1. Namely, they assume that initially spherical particles of the same radius R simultaneously form during the plastic deformation a neck of a parabolic profile, as illustrated in Fig. 2. The current radius of the bridging cross section of a particle r, the vertical coordinate of the intersection of the parabolic neck with the undisturbed spherical portion of a particle y_{pn} and the half of the crack opening displacement at the particle site $\Delta/2$ within the bridging zone are then related by

$$\frac{r}{R} = \sqrt{1 - \left(\frac{y_{pn}}{R} - \frac{\Delta(\rho)}{2R}\right)^2} - \frac{\kappa}{2}\left(\frac{y_{pn}}{R}\right)^2 , \tag{1}$$

where κ is the curvature of the chosen parabolic profile, $x'/R = \kappa\,(y/R)^2\,/2 + r/R$. Rubinstein and Wang [1] suggest to associate this parameter with the strength of the matrix/particle interface and to use it as a parameter of the composite. The requirement of incompressibility of the particles provides then the additional condition for determination

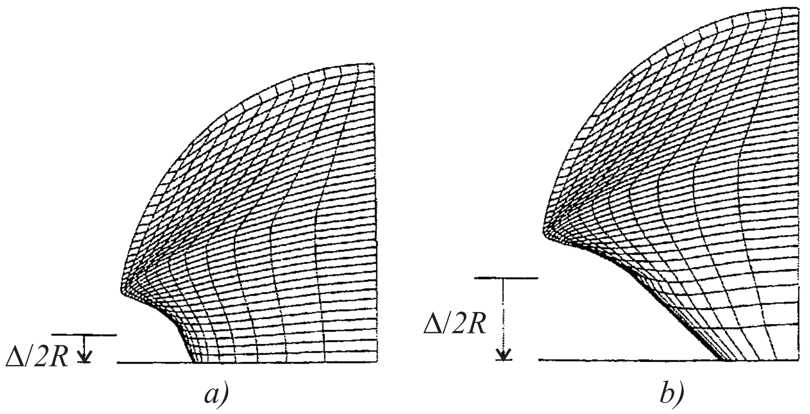

Fig. 1: Sketch of the deformed mesh pertaining to the FE simulation of constrained particle according to Tvergaard [7].

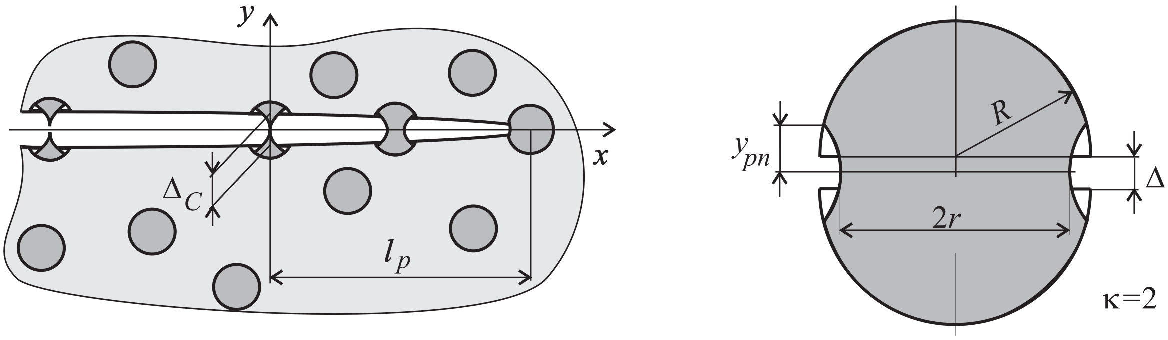

Fig. 2: Scheme of bridged crack and particle deformation shape for $\kappa = 2$.

of r, y_{pn}, and $\Delta/2$:

$$
\begin{aligned}
2 \;=\; & \left(1 - \frac{y_{pn}}{R} + \frac{\Delta(\rho)}{2R}\right)^2 \left(2 + \frac{y_{pn}}{R} - \frac{\Delta(\rho)}{2R}\right) \\
+ \; & 3\left[\frac{\kappa^2}{20}\left(\frac{y_{pn}}{R}\right)^2 + \frac{\kappa}{3}\frac{r}{R}\left(\frac{y_{pn}}{R}\right)^3 + \frac{y_{pn}}{R}\left(\frac{r}{R}\right)^2\right].
\end{aligned} \tag{2}
$$

A significant simplification was introduced by assuming a constant stress within the bridging section of each particle.

In this paper we will make use of Eqs. (1) and (2) for analytical modelling of debonding of matrix/particle interface. The mean axial stress in the necked bridging section of particles is, however, assumed not to be constant but given by Bridgman's solution. The condition of a critical particle stretching $\Delta = \Delta_C$, which controls the ligaments rupture, is imposed. The action of the system of discretely distributed particles is replaced by the action of smeared forces over the bridged zone length l_p. Small scale bridging is assumed, i.e. $l_p << a$, where a is the crack length. Thus, a semi-infinite crack, $x < 0$, $y = 0$, may be considered. The remote load is given through the boundary layer approach, so that the stress $\sigma_{yy} = K_I^N/\sqrt{2\pi x}$ for $x >> l_p$, $y = 0$, where K_I^N is the remote stress intensity factor which can be found by solving an appropriate boundary value problem on the macrolevel using e.g. FEM. Because the bridged zone is situated in an essentially elastic environment, there is also an inner, or so called local stress intensity factor K_I^{loc}, pertinent to the crack edge vicinity. Obviously, K_I^{loc} is smaller than K_I^N. The material behaviour outside the bridging zone is homogeneous, linear elastic and the elastic properties may be determined on the basis of a mixture rule which may account for the presence of lower stiffness particles. The applied procedure allows one to obtain a nonlinear integral equation which has to be solved numerically. Recently a powerful solution technique for solving bridged crack problems has become widely used, see e.g. Ioakimidis [11], Kaya and Erdogan [12] and Nemat-Nasser and Hori [13]. This technique is based on a mathematical formalism which involves integral equations with a stronger singularity than the Cauchy type. The improper strongly singular integrals are treated in the Hadamard sense [14] of their "finite part".

MATHEMATICAL MODELLING

The continuously distributed crack surface bridging load σ_0 can be determined as follows: if R is the average particle radius, l is the interparticle distance and f is the volume fraction of particles, then the restraining stress σ_0 is found to be $\sigma_0 = P/l^2 = P/R^2\,(3f/4\pi)^{2/3}$, where P is the bridging force of a single particle. The bridging force P relates to the mean axial stress σ_1 in the necked region of a particle and to the current radius of the bridging cross section of a particle r as $P = \pi r^2 \sigma_1$. The mean axial stress σ_1 is estimated from Bridgman's solution, see also Bao [6]:

$$\sigma_1 = \sigma_f \left(1 + \frac{2R}{\kappa r}\right) \ln\left(1 + \frac{\kappa r}{2R}\right) , \tag{3}$$

where σ_f is the uniaxial flow stress of the ductile particle. It should be noted that the Bridgman formulae somewhat underestimates the elevation of the mean and axial stresses in the neck region. If a power law hardening material is assumed, then the σ_f is related to the tensile strain e by $\sigma_f/\sigma_y = (e/e_y)^n$, where σ_y and e_y are the initial yielding stress and strain respectively and n is the hardening coefficient. The value of e_y was considered 0.002 according to Tvergaard [8]. The tensile strain e relates to the initial particle radius and to the current radius of bridging cross section by

$$e = 2\ln\left(R/r\right) . \tag{4}$$

Finally, the restraining stress σ_0 can be estimated as

$$\sigma_0 = 2^n e_y^{-n} \sigma_y \left(\frac{3f\sqrt{\pi}}{4}\right)^{2/3} \left[\ln\left(\frac{R}{r}\right)\right]^n \left(\frac{r}{R}\right)^2 \left(1 + \frac{2R}{\kappa r}\right) \ln\left(1 + \frac{\kappa r}{2R}\right) . \tag{5}$$

In order to obtain the restraining stress σ_0 as a function of the normalized crack opening displacement Δ/R within the bridging zone for the specified curvature of the chosen parabolic profile of the particle's neck, the normalized vertical coordinate y_{pn}/R of the intersection of the parabolic neck with the undisturbed spherical portion of a particle is first eliminated between Eqs. (1) and (2) and the normalized current radius of the bridging cross section r/R is expressed as a function of Δ/R. Fig. 3 shows the plots of the bridging cross section r/R against Δ/R for several values of the curvature κ of the chosen parabolic profile of the particle's neck. If the relation $r/R - \Delta/R$ is substituted into (5) a desired function $\sigma_0\,(\Delta/R)$ is obtained. Fig. 3 shows the course of the normalized restraining stress $\sigma_0/[\sigma_y\,(3f\sqrt{\pi}/4)^{2/3}]$ vs. the normalized crack opening displacement Δ/R for several values of the curvature κ for ideally plastic material. Plots in Fig. 4 indicate that the slope of $\sigma_0\,(\Delta/R)$ curve is negative in the stage of the plastic deformation of bridging particles and

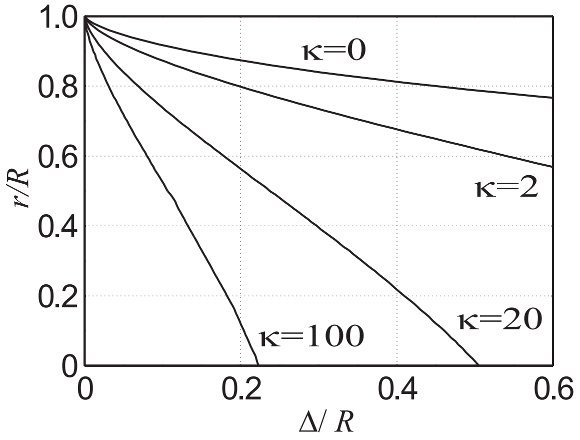

Fig. 3: Plots of the bridging cross section r/R against Δ/R for several values of κ.

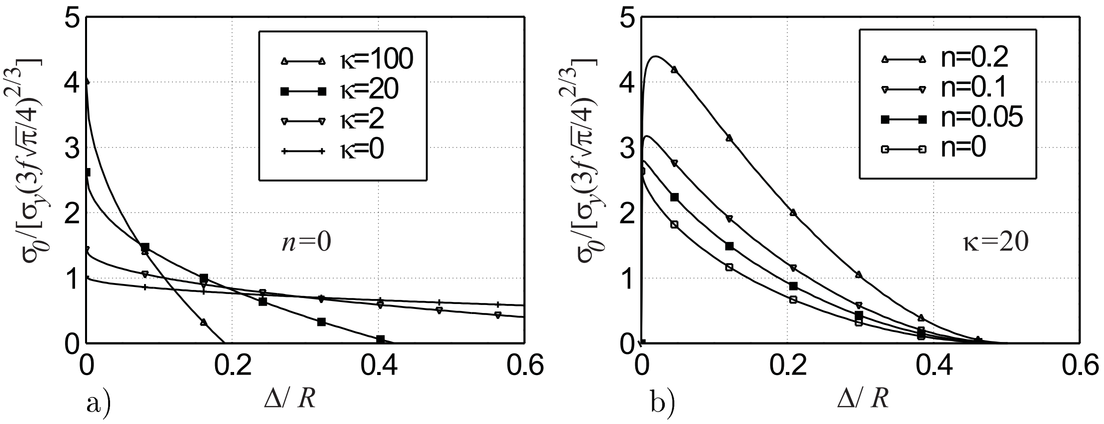

Fig. 4: Plots of the normalized restraining stress vs. Δ/R; a) for several values of κ and $n = 0$, b) for $\kappa = 20$ and several values of n.

the bridging zone here exhibits softening behaviour. For the purpose of further analysis there is convenient to have a simple mathematical approximation of the curves in Fig. 4. Using the method of least squares these curves were fitted to the function linear in $\sqrt{\Delta/R}$, i.e.

$$\sigma_0/[2^n e_y^{-n}\sigma_y(3f\sqrt{\pi}/4)^{2/3}] \doteq -c_1\sqrt{\Delta/R}+c_2, \quad (c_1>0,\ c_2>0). \tag{6}$$

Individual fits are not shown in Fig. 4 because they are barely distinguishable from the exact numerical curves. The square root dependence of the normalized restraining stress upon the crack opening displacement in Eq. (6) allows to use a simple perturbation method to the solution of the resulting singular integral equation as it will be seen later on.

The analytical formulation is based on the distribution dislocation technique, see Hills *et al.* [17], and the boundary layer approach through which the remote load is introduced. The dislocation distribution is introduced only along the bridging zone, the traction-free crack faces are modelled via mirror stresses. The equilibrium condition across the bridging zone leads to the following singular integral equation for the unknown Burgers vector density $b_y(x)$

$$\frac{K_I^N}{\sqrt{2\pi}}+\frac{E}{8\pi(1-\nu^2)}\left[\fint_0^{l_p}\frac{b_y(x')}{\sqrt{x}-\sqrt{x'}}\,\mathrm{d}x'-\int_0^{l_p}\frac{b_y(x')}{\sqrt{x}+\sqrt{x'}}\,\mathrm{d}x'\right]=\sigma_0\sqrt{x}, \tag{7}$$

where E is the Young modulus and ν Poisson's ratio of composite, the symbol $⨍$ represents the Cauchy principal value. The Burgers vector density function $b_y(x)$ is related to the displacement-discontinuity across the bridging zone $\Delta(x')$ by

$$b_y(x') = -\mathrm{d}\Delta(x')/\mathrm{d}x'. \tag{8}$$

By setting

$$\rho = 2\sqrt{x/l_p} - 1, \quad \rho' = 2\sqrt{x'/l_p} - 1, \tag{9}$$

the square roots in (7) can be removed and simultaneously the integration interval can be normalized to $<-1, 1>$. Eq. (8) provides after the transformation (9):

$$b_y(x') = -\frac{2}{l_p(\rho'+1)}\frac{\mathrm{d}\Delta[l_p(\rho'+1)^2/4]}{\mathrm{d}\rho'} = -\frac{2}{l_p(\rho'+1)}\frac{\mathrm{d}\Delta^*(\rho')}{\mathrm{d}\rho'}\,. \tag{10}$$

Substituting (10) into the transformed Eq. (7) we obtain a singular integral equation for unknown derivative of the jump of displacement component as follows

$$\begin{aligned} &⨍_{-1}^{1} \frac{1}{(\rho-\rho')}\frac{\mathrm{d}\Delta^*(\rho')}{\mathrm{d}\rho'}\,\mathrm{d}\rho' - \int_{-1}^{1} \frac{1}{(\rho'+\rho+2)}\frac{\mathrm{d}\Delta^*(\rho')}{\mathrm{d}\rho'}\,\mathrm{d}\rho' = \\ = \;& -\frac{2(1-\nu^2)}{E}\left[\sqrt{2\pi}\sqrt{l_p}K_I^N - \pi(\rho+1)\,l_p\,\sigma_0\right]. \end{aligned} \tag{11}$$

Integrating Eq. (11) by part and using an apparent condition at the crack tip $\Delta^*(\rho' = 1) \equiv 0$, we can reduce this equation to

$$\text{⨎}_{-1}^{1} \frac{\Delta^*(\rho')}{(\rho'-\rho)^2}\,\mathrm{d}\rho' + \int_{-1}^{1} \frac{\Delta^*(\rho')}{(\rho'+\rho+2)^2}\,\mathrm{d}\rho' = -\frac{2(1-\nu^2)}{E}\left[\sqrt{2\pi}\sqrt{l_p}K_I^N - \pi(\rho+1)\,l_p\,\sigma_0\right], \tag{12}$$

where the symbol ⨎ denotes the finite part of the improper (strongly singular) integral in the sense of Hadamard [14]. If Eq. (12) is divided by the particle radius R and $\Delta^*(\rho')$ is formally denoted again by $\Delta(\rho')$, we obtain a strongly singular integral equation for the normalized crack opening displacement $\Delta(\rho)/R$, $\rho \in <-1, 1>$

$$\begin{aligned} &\text{⨎}_{-1}^{1} \frac{1}{(\rho'-\rho)^2}\frac{\Delta(\rho')}{R}\,\mathrm{d}\rho' + \int_{-1}^{1} \frac{1}{(\rho'+\rho+2)^2}\frac{\Delta(\rho')}{R}\,\mathrm{d}\rho' = \\ = \;& -\frac{2(1-\nu^2)}{ER}\left[\sqrt{2\pi}\sqrt{l_p}K_I^N - \pi(\rho+1)\,l_p\,\sigma_0(\Delta(\rho)/R)\right]. \end{aligned} \tag{13}$$

NUMERICAL SOLUTION

Substitute the fit of the restraining stress $\sigma_0[\Delta(\rho)/R]$ from Eq. (6) in Eq. (13) and rewrite it formally in the following form

$$L_{-1}^{1}[\Delta(\rho)/R] + \varepsilon\Lambda(\rho)\sqrt{\Delta(\rho)/R} = \Lambda'(\rho), \tag{14}$$

where L_{-1}^{1} is the integral operator defined by

$$L_{-1}^{1}\left[\frac{\Delta(\rho)}{R}\right] = \text{⨎}_{-1}^{1} \frac{1}{(\rho'-\rho)^2}\frac{\Delta(\rho')}{R}\,\mathrm{d}\rho' + \int_{-1}^{1} \frac{1}{(\rho'+\rho+2)^2}\frac{\Delta(\rho')}{R}\,\mathrm{d}\rho'\,, \tag{15}$$

$\Lambda(\rho)$ and $\Lambda'(\rho)$ are linear functions

$$\Lambda(\rho) = c_1(\rho+1), \quad \Lambda'(\rho) = \varepsilon c_2(\rho+1) - \lambda\,, \tag{16}$$

where

$$\varepsilon = \frac{2\pi(1-\nu^2)}{E}\, 2^n e_y^{-n} \sigma_y (3f\sqrt{\pi}/4)^{2/3} \frac{l_p}{R}, \quad \lambda = \frac{2(1-\nu^2)}{E}\sqrt{2\pi}\frac{\sqrt{l_p}}{R} K_I^N \tag{17}$$

which, in a wide range of typical values of materials properties, fulfills the inequality $\varepsilon < 1$. The singular integral equation of the type of (14) was intensively investigated in Nemat-Nasser and Hori [13] and Willis and Nemat-Nasser [16]. For $\varepsilon < 1$ an asymptotic expansion of $\Delta(\rho)/R$ in terms of ε can be considered

$$\Delta(\rho)/R \cong \sum_{p=0}^{N} \varepsilon^p \phi_p(\rho)/R\,, \quad \phi_p(\rho) = 0 \text{ for } \rho = 1\,, \tag{18}$$

where N is a suitable large positive integer. It is further convenient to rewrite Eq. (14) as

$$\varepsilon^2 \Lambda^2(\rho)\Delta(\rho)/R = \Lambda'(\rho) - L_{-1}^1[\Delta(\rho)/R]^2\,. \tag{19}$$

Substituting Eq. (18) into Eq. (19) and rearranging terms, the following system of recursive linear singular equations for the coefficients of the corresponding powers of the parameter ε in the asymptotic expansion (18) is obtained:

$$\begin{aligned}
L_{-1}^1[\phi_0(\rho)/R] &= -\lambda\,, \quad L_{-1}^1[\phi_1(\rho)/R] = \rho + 1 + \Lambda(\rho)\sqrt{\lambda}\,\phi_0(\rho)/R\,,\\
L_{-1}^1[\phi_2(\rho)/R] &= \frac{\Lambda(\rho)\,\phi_1(\rho)/R}{2\sqrt{\phi_0(\rho)/R}}\,,\\
L_{-1}^1[\phi_p(\rho)/R] &= \frac{\Lambda^2(\rho)\,\phi_{p-1}(\rho)/R - \sum_{m=2}^{p-1} L_{-1}^1[\phi_m(\rho)/R]\,L_{-1}^1[\phi_{p+1-m}(\rho)/R]}{2\Lambda(\rho)\sqrt{\phi_0(\rho)/R}}\,,\\
p &= 3\,, 4\,, \ldots
\end{aligned} \tag{20}$$

Solutions of the recursive linear singular equations (20) may be expressed according to Kaya [12] in the form $\phi_p(\rho) = F_p(\rho)w(\rho)$, where F_p is unknown bounded function and $w(\rho)$ is fundamental (or weight) function determined by the nature of corresponding mixed-boundary value problem. At the present case $w(\rho) = \sqrt{1-\rho}$. The unknown function F_p is approximated by a truncated series as

$$F_p(\rho) \cong \sum_{j=0}^{s} a_{pj}\rho^j\,, \tag{21}$$

and the coefficients a_{pj} are determined by a simple collocation method. Numerical results and our previous experiences with the method [18] indicate that the convergence of the collocation method is very good so that it is sufficient to set $s = 6$ in the series (21). The influence of the number of terms in the asymptotic expansion of $\Delta(\rho)/R$ in Eq. (18) is illustrated in Fig. 5 which shows a change of the crack opening displacement along the bridging zone as the number of terms in (18) increases for specified values of composite parameters and two values of the critical normalized crack opening displacement Δ_C/R. The value of the parameter ε is predominantly determined by the normalized length l_p/R of the bridging zone which can change in a wide range. Note that the ratio of the yield stress over the elastic modulus is not expected to vary significantly for different composite

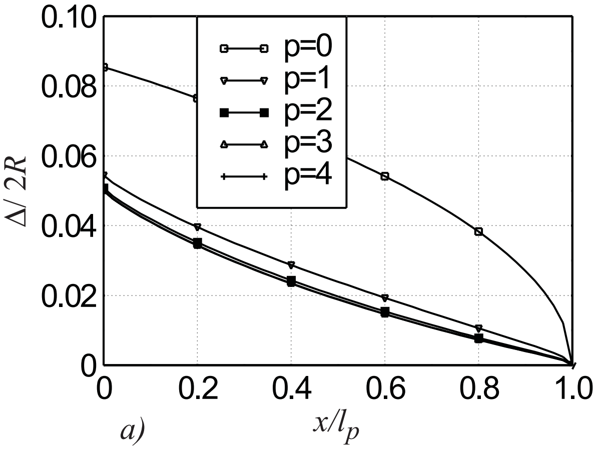

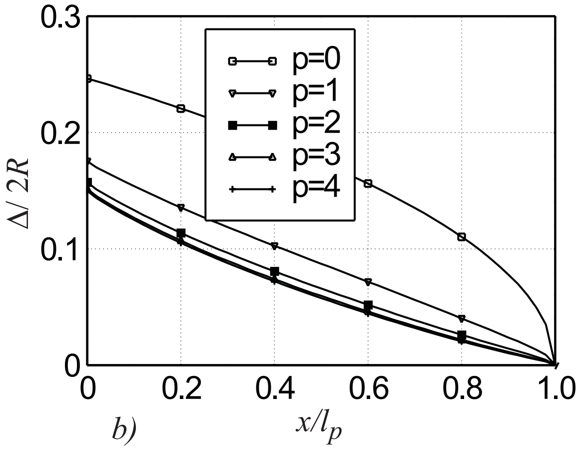

Fig. 5: Change of the half of the normalized half-crack opening displacement along the bridging zone as the number of terms in (18) increases for $k = 0.5$, $f = 0.25$, $n = 0$, $\nu = 0.2$, $\kappa = 2$ and a) $\Delta_C/R = 0.1$, b) $\Delta_C/R = 0.3$.

systems and is set to a reasonable value of 0.001. The convergence is very good up to the value of $l_p/R = 325$. It will be shown later on that these values are never reached before the failure of particles in the bridging zone occurs.

Once the solution is obtained, the local stress intensity factor K_I^{loc} is determined using the standard formula, see Kotoul a Urbiš [18]:

$$\begin{aligned} K_I^{loc} &= \frac{E}{2(1-\nu^2)} \lim_{\rho\to 1^-} \frac{\sqrt{\pi}\Delta(\rho)}{\sqrt{2l_p(1-\rho)(\rho+3)}} \\ &= \frac{K_{IC}}{8(1-\nu^2)} \frac{E}{\sigma_y} \frac{1}{k} \lim_{\rho\to 1^-} \frac{\pi\Delta(\rho)/R}{\sqrt{(1-\rho)(\rho+3)l_p/R}}, \end{aligned} \tag{22}$$

where K_{IC} is the fracture toughness of the matrix and $k = \frac{K_{IC}}{2\sigma_y}\sqrt{\frac{\pi}{2R}}$ is another composite parameter which combines the fracture toughness of the matrix with the yield strength and the radius of the particles. Note that its mathematical structure is of the form of ratio of the fracture toughness of the matrix and the restraining stress intensity factor corresponding to the bridging zone of the length $2R$ and the strength σ_y. Crack growth in the matrix is controlled by the value of the local stress intensity factor; it has to reach the critical value for the matrix K_{IC}

$$K_I^{loc} = K_{IC}\,. \tag{23}$$

The bridged zone length l_p is controlled by the crack opening displacement which has to reach a critical value Δ_C for the rupture of most stretched ligaments would take place

$$\Delta = \Delta_C\,. \tag{24}$$

Formally, the conditions (23) and (24) can be written as

$$F_i\left(\frac{K_I^N}{K_{IC}}, \frac{l_p}{R}; k, \frac{\Delta_C}{R}, f, n, \frac{\sigma_y}{E}, \nu\right) = 0, \quad i = 1, 2, \tag{25}$$

where F_i are nonlinear functions of variables K_I^N/K_{IC} and l_p/R while κ, k, Δ_C/R, n, f, σ_y/E and ν belong to the set of dimensionless parameters upon which the solution depends. The parameters κ , k , Δ_C/R, and f, are of principal importance while the parameters σ_y/E and ν are treated as secondary ones because, in spite of they do influence the reinforcing mechanism by affecting the crack opening displacement, the change of the particle shape and the bridging particle cross section, they do not vary significantly for different composites and thus they are not included in the parametric study.

NUMERICAL RESULTS AND DISCUSSION

Equations (25) has been solved for unknowns K_I^N/K_{IC} and l_p/R with various combinations of the parameters κ , k , Δ_C/R , n , f , σ_y/E and ν . The solution for K_I^N/K_{IC} is denoted by $(K_I^N/K_{IC})_{eff}$. This value, which is called the normalized effective fracture toughness of composite, describes the toughening effect of ductile particles. Basing on Eqs. (25) a relationship among the effective fracture resistance and the parameters κ , k , Δ_C/R , f , σ_y/E and ν can be studied.
In order to display the numerical results in most comprehensible form which allows to make comparison with some previous results reported elsewhere, the following strategy is adopted; for a given value of the curvature κ the unknowns K_I^N/K_{IC} and l_p/R are calculated as functions of the normalized critical crack opening displacement Δ_C/R on a interval $0 < \Delta_C/R \leq \Delta_{\max}/R$, where $\Delta_{\max}/R$ is the intercept of the $\sigma_0 - \Delta/R$ relation with the Δ/R axis, see Fig. 4. These calculations are performed for several values of the volume fraction of particles f and the composite parameter k. Thus, for each value of Δ_C/R (with f , n and k held constant) a pair of values of $(K_I^N/K_{IC})_{eff}$ and l_p/R is obtained which allows to plot $(K_I^N/K_{IC})_{eff}$ against l_p/R by changing Δ_C/R. The plots are shown in Figs 6-7. Note that with f held constant a higher value of the composite fracture resistance is predicted with decreasing value of the parameter k , i.e. with increasing the size of particles in a specified material system. The same trend was predicted by Rubinstein and Wang [1]. An increase in the composite fracture resistance due to the hardening exponent increase is also apparent. This effect, however, becomes weaker with decreasing debonding of particles, i.e. with increasing value of the curvature κ.

So far the critical crack opening displacement Δ_C/R has been treated as an independent model parameter and has changed arbitrarily within the interval $(0, \Delta_{\max}/R >$. However, one should realize that Δ_c/R depends on the particle ductility and the stress triaxiality as well. The latter is governed by the curvature κ of the chosen parabolic profile and associates with the strength of the matrix/particle interface. In order to compare an increase in the toughness $(K_I^N/K_{IC})_{eff}$ for different κ, the stress triaxiality factor in bridging particles should be included. To do this, a rupture criterion of bridging particles has to be formulated. Assume that microvoids are nucleated on micro-inhomogeneities in the necked region of a bridging particle and rupture occurs when the neighbouring microvoids come into contact. Widely used in the local approach of ductile fracture is the criterion based on the Rice and Tracey [19] equation for the growth of an initially spherical void. On integrating this equation with the assumption that stress state remains constant and there is no void nucleation strain, the equivalent fracture strain $\overline{e}_{fr}$ is given by

$$\overline{e}_{fr} = \frac{\ln[(\overline{d}_p)/(2\overline{r})]}{0.28\ \exp\left[(3\,\sigma_m)/(2\,\sigma_{eq})\right]}\,, \tag{26}$$

where σ_m is the hydrostatic stress, σ_{eq} is von Mises equivalent stress and $\overline{d}_p$ and $\overline{r}$ stand for the mean spacing and the mean radius of inhomogeneities respectively. For a uniaxial

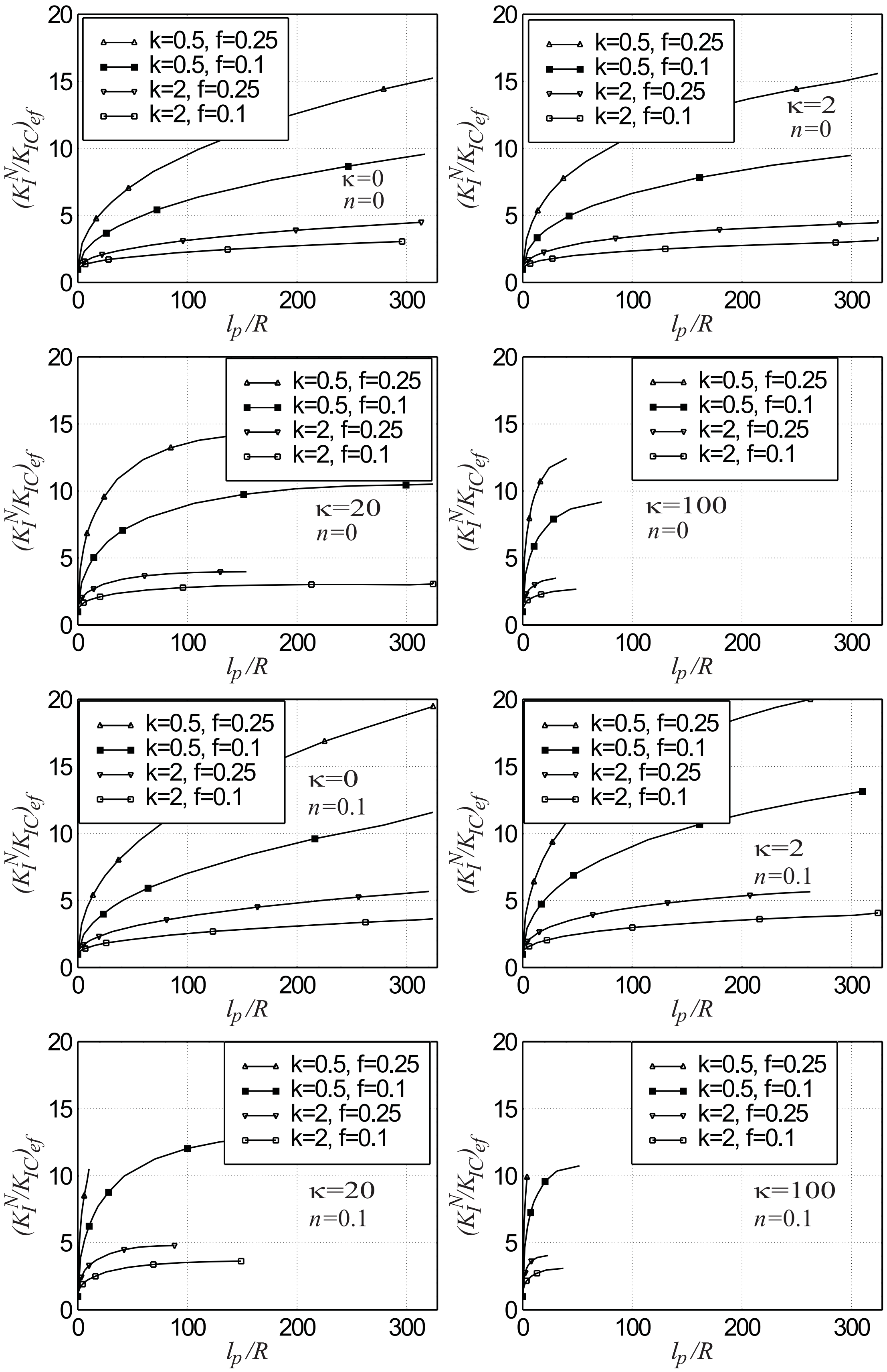

Fig. 6: Plots of the normalized effective fracture toughness $\left(K_I^N/K_{IC}\right)_{ef}$ vs. the normalized length of the bridged zone l_p/R for $\nu = 0.2$ and several values of k , f , n and κ.

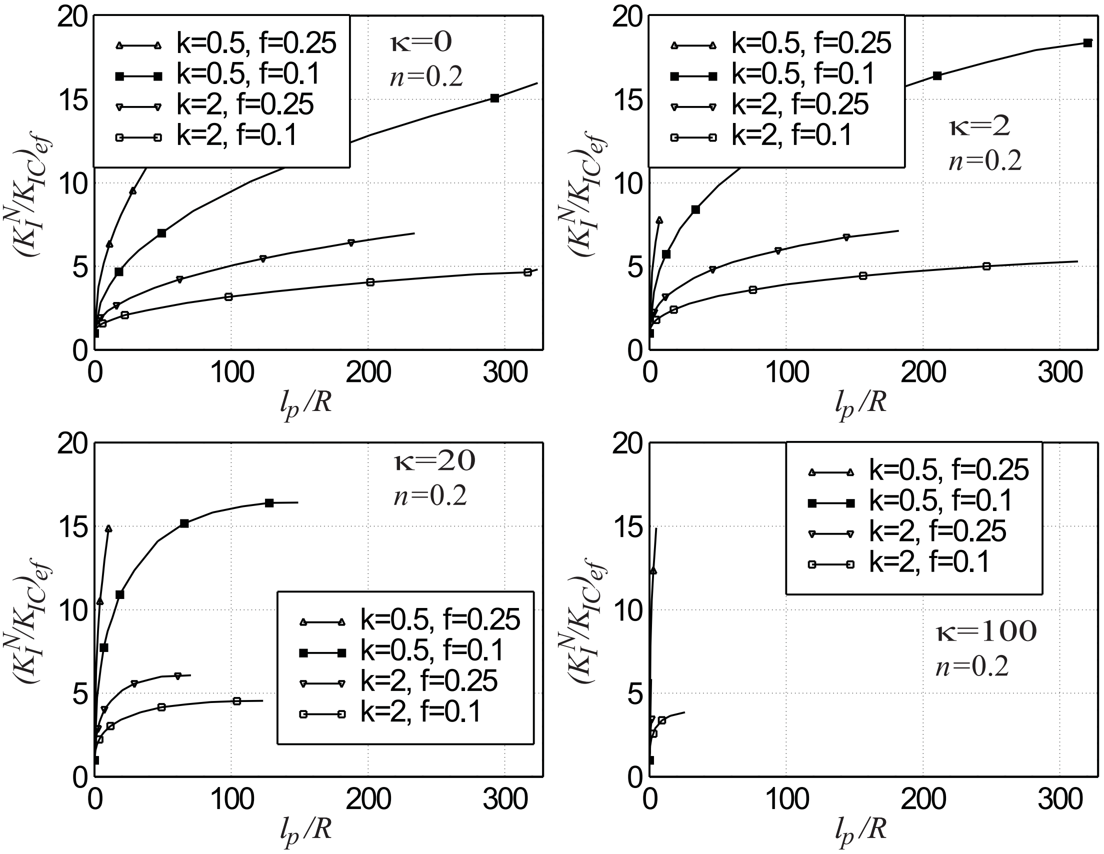

Fig. 7: Plots of the normalized effective fracture toughness $\left(K_I^N/K_{IC}\right)_{ef}$ vs. the normalized length of the bridged zone l_p/R for $\nu = 0.2$ and several values of k, f, κ and $n = 0.2$.

stress state, which exists in the ligaments with $\kappa = 0$, the ratio σ_m/σ_f is $1/3$. The absolute value of the fracture strain is not matter of interest because we intend only to compare the fracture strains of bridging particles with different curvature of the parabolic neck profile, i.e. with different stress triaxiality factor σ_m/σ_f. Thus, the knowledge of the microstructural parameter $\overline{d}_p/2\overline{p}$ is not essential. We proceed as follows: the equivalent fracture strain $\overline{e}_{fr}$ can be related to the initial particle radius and to the current radius of bridging cross section by (4). In the case $\kappa = 0$ Eq. (26) reads

$$2\ln\left[\left(\frac{R}{r}\right)_{\kappa=0}\right]_{fr} = \frac{\ln[(\overline{d}_p)/(2\overline{r})]}{0.28\ \exp\left(1/2\right)}\,. \tag{27}$$

Eqs. (1) and (2) provide the relation $r/R = f(\Delta/R)$, see Fig. 3, which allows to rewrite Eq. (27) in the form

$$2\ln\left(\frac{1}{f(\Delta_C/R)_{\kappa=0}}\right) = \frac{\ln[(\overline{d}_p)/(2\overline{r})]}{0.28\ \exp\left(1/2\right)}\,. \tag{28}$$

Eq. (28) gives the value of the critical crack opening displacement Δ_C/R for $\kappa = 0$. Assume now the case $\kappa > 0$. Then using Eq. (3) and $\sigma_m/\sigma_f = \sigma_1/\sigma_f - 2/3$ one obtains

$$2\ln\left[\left(\frac{R}{r}\right)_{\kappa\neq0}\right]_{fr} = \frac{\ln[(\overline{d}_p)/(2\overline{r})]}{0.28\ \exp\left[\frac{3}{2}\left(1+\frac{2R}{\kappa r}\right)\ln\left(1+\frac{\kappa r}{2R}\right)-1\right]}\,, \tag{29}$$

or, making use of Eq.(28)

$$\ln\left[\left(\frac{R}{r}\right)_{\kappa\neq 0}\right]_{fr} = \ln\left(\frac{1}{f(\Delta_C/R)_{\kappa=0}}\right)\frac{\exp(1/2)}{\exp\left[\frac{3}{2}\left(1+\frac{2R}{\kappa r}\right)\ln\left(1+\frac{\kappa r}{2R}\right)-1\right]}\,. \tag{30}$$

Note, that for a chosen value of $(\Delta_C/R)_{\kappa=0}$ and the specified curvature κ one can solve Eq. (30) for r/R and find the critical crack opening displacement $(\Delta_C/R)_{\kappa>0}$ from the relation $r/R = f(\Delta/R)$, see Fig. 3. The results of these computations are given in Fig. 8 which illustrates the relation between $(\Delta_C/R)_{\kappa>0}$ and $(\Delta_C/R)_{\kappa=0}$ for several values of the curvature κ. Fig. 8 indicates that the critical crack opening displacement $(\Delta_C/R)_{\kappa>0}$ is significantly reduced for higher values of the curvature κ comparing to the critical crack opening displacement $(\Delta_C/R)_{\kappa=0}$ due to the influence of the stress triaxiality factor.

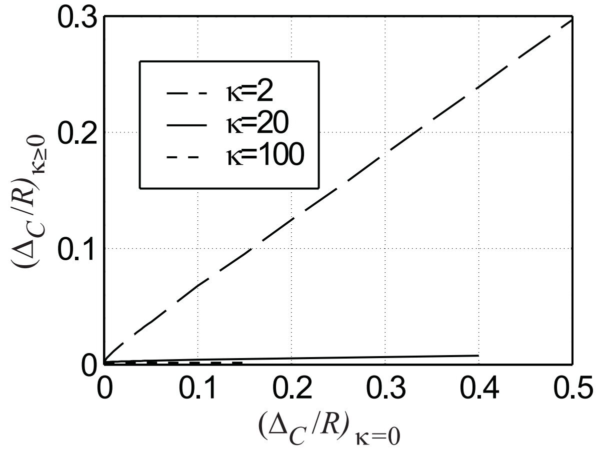

Fig. 8: Relation between the critical half-crack opening displacements $(\Delta_C/R)_{\kappa>0}$ and $(\Delta_C/R)_{\kappa=0}$ for several values of the curvature κ.

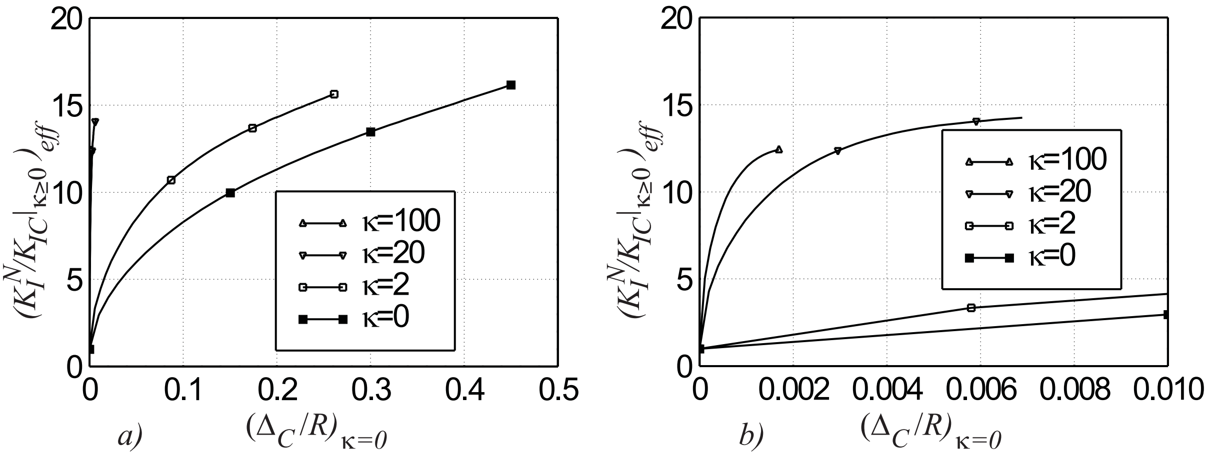

Fig. 9: Relation $(K_I^N/K_{IC}\,|_{\kappa\geq 0})_{eff}$ vs. $(\Delta_C/R)_{\kappa=0}$ including also the effect of the stress triaxiality factor upon the critical crack opening displacement, $k=0.5$, $f=0.25$, $n=0$, $\nu=0.2$ a) full scale diagram, b) zoomed detail of the left section of the diagram a).

Now we are in position to compare an increase in the toughness $(K_I^N/K_{IC})_{eff}$ for different values of the curvature κ including also the effect of the stress triaxiality factor upon the critical crack opening displacement. Namely, the results in Fig. 6 together with the previous computations of $(K_I^N/K_{IC})_{eff}$ from Eqs. (25) provide us with the relation $(K_I^N/K_{IC}\ |_{\kappa\geq 0})_{eff}$ vs. $(\Delta_C/R)_{\kappa=0}$ as displayed in Fig. 9. $(\Delta_C/R)_{\kappa=0}$ serves as an independent variable which characterizes the ductility of bridging particles under the uniaxial stress state condition. Fig. 9 reveals two counteracting influences of the matric/particle interface strength. The cases of weak interface, i.e. low values of the curvature κ , allow for higher value of the critical crack opening displacement which entails an increase in the fracture resistance of composite; however, due to the low stress triaxiality in this case, the restraining stress σ_0 is rather low, see Fig. 4 and, consequently, the restraining stress intensity factor is also low which reduces the fracture resistance of composite. On the other side, high values of the curvature κ introduce a significant level of the stress triaxiality in bridging particles which promotes the high restraining stress σ_0 and thus increases the fracture resistance; simultaneously however, the critical crack opening displacement rapidly drops and the energy absorbed in the particle rupture falls down thus decreasing the fracture resistance of composite.

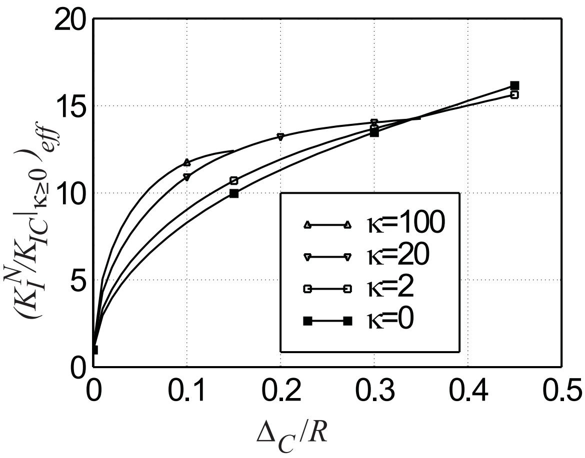

Fig. 10: Fracture resistance curves $(K_I^N/K_{IC}\ |_{\kappa\geq 0})_{eff}$ vs. (Δ_C/R) , $k=0.5$, $f=0.25$, $n=0$, $\nu=0.2$; the effect of the stress triaxiality upon the critical crack opening displacement is not considered.

For comparison, Fig. 10 shows results of the computation of the fracture resistance curves $(K_I^N/K_{IC}\ |_{\kappa\geq 0})_{eff}$ vs. (Δ_C/R), where the effect of the stress triaxiality factor upon the critical crack opening displacement is not considered and Δ_C/R changes in the interval $(0,\Delta_{\max}/R>$, where as already noted, $\Delta_{\max}/R$ denotes the intercept of the $\sigma_0-\Delta/R$ relation with the Δ/R axis. Summarizing, a certain optimal interfacial debonding, which closely relates to the unconstrained particle ductility characterized by the parameter $(\Delta_C/R)_{\kappa=0}$, is required to achieve an optimal fracture toughness of composite. At the same time, Fig. 9 indicates that the optimal property for the interface is not necessary the case of the curvature $\kappa=0$ as stated in Rubinstein and Wang [1] and Venkateswara *et al.* [10].

REFERENCES

[1] Rubinstein, A. A. and Wang, P.: *J. Mech. Phys. Solids* **46**, (1998), pp. 1139–1154.

[2] Rose, L. R. F.: *J. Mech. Phys. Solids* **35**, (1987), pp. 383–405.

[3] Budiansky, B.: Micromechanics II, in Proc. of the 10th U.S. National Congress of Applied Mechanics, Austin (Ed.), ASME, New York, 1996, pp. 25–32.

[4] Budiansky, B., Amazigo, J. and Evans, A. G.: *J. Mech. Phys. Solids* **36**, (1987), pp. 167–167.

[5] Erdogan, F. and Joseph, P. F.: *J. Am. Ceram. Soc.* **72**, (1989), pp. 262–270.

[6] Bao, G. and Hui, C-Y.: *Int. J. Solids Structures* **26**, (1990), pp. 631–642.

[7] Tvergaard, V.: *Int. J. Mech. Sci.* **34**, (1992), pp. 635–649.

[8] Tvergaard, V.: In: *Fracture of Brittle Disordered Materials: Concrete, Rock and Ceramics* G. Baker and B. L. Karihaloo (Ed.), F&F. N. Spon, London, U.K. 1995, 361–375.

[9] Sigl, L.S., Mataga, P.A., Dalgleish, B.J., McMeeking, R.M, and Evans, A.G.: *Acta Metallurgica* **36**, (1988), pp. 945–953.

[10] Venkateswara Rao, K.T., Soboyejo, W.O. and Ritchie, R.O.: *Metallurgical Transactions A* **23A**, (1992), pp. 2249–2257.

[11] Ioakimidis, N. I.: *Acta Mechanica* **45**, (1982), pp. 31–47.

[12] Kaya, A. C. and Erdogan, F.: *Quarterly of Appl. Mathematics* **XLV**, (1987), pp. 105–122.

[13] Nemat-Nasser, S. and Hori, M.: *Mechanics of Materials* **6**, (1987), pp. 245–269.

[14] Hadamard, J.: Lectures on Cauchy's Problem in Linear Partial Differential Equations. New York: Dover, 1952.

[15] Hori, M. and Nemat-Nasser, S.: *SIAM Journal of Appl. Mathematics* **50**, (1990), pp. 716–725.

[16] Willis, J. R. and Nemat-Nasser S.: *Quarterly of Appl. Mathematics* **XLVIII**, (1990), pp. 741–753.

[17] Hills, D. A., Kelly, P. A., Dai, D. N. and Korsunsky, A. M.: Solution of crack problems: The distributed dislocation technique. Dordrecht: Kluwer Academic Publishers, 1996.

[18] Kotoul, M. and Urbiš, R.: *Eng. Frac. Mechanics*, **68**, (2000), pp. 89–105.

[19] Rice, J. R. and Tracey, D. M.: *J. Mech. Phys. Solids*, **17**, (1969), pp. 201–217.